Ships and Offshore Structures

ISSN: (Print) (Online) Journal homepage: https://www.tandfonline.com/loi/tsos20

Route planning for autonomous vessels based on improved artificial fish swarm algorithm

Liang Zhao, Fang Wang & Yong Bai

To cite this article: Liang Zhao, Fang Wang & Yong Bai (2022): Route planning for autonomous vessels based on improved artificial fish swarm algorithm, Ships and Offshore Structures, DOI: 10.1080/17445302.2022.2081423

To link to this article: https://doi.org/10.1080/17445302.2022.2081423

SHIPS AND OFFSHORE STRUCTURES
https://doi.org/10.1080/17445302.2022.2081423

Taylor & Francis
Taylor & Francis Group

Route planning for autonomous vessels based on improved artificial fish swarm algorithm

Liang Zhao[a], Fang Wang[b] and Yong Bai[a]

[a]School of Civil Engineering and Architecture, Zhejiang University, Hangzhou, People's Republic of China; [b]School of Information and Electrical Engineering, Zhejiang University City College, Hangzhou, People's Republic of China

ABSTRACT

Path planning is one of the key technologies in the research of autonomous surface vessels (ASVs). In this paper, an improved artificial fish swarm algorithm (IAFSA) is proposed. The algorithm is modified from four perspectives: (1) A directional operator is introduced to improve the efficiency. (2) To avoid local optimum, a probability weight factor is proposed to adjust the frequency of executing random behaviour. (3) An adaptive operator has been applied aims at better convergence performance. (4) The waypoint modifying path smoother is used to improve the path quality. A comparative study has been carried out between IAFSA and the other state-of-the-art algorithms, and the results indicate that the proposed algorithm outperforms the others in both efficiency and path quality. Finally, IAFSA is integrated into the GNC system in a model ship. A computer-based sea trial around the Nan Hai area has been conducted, and environmental disturbances including wind, waves, and currents are considered. The results have shown that IAFSA is suitable for practical application.

ARTICLE HISTORY
Received 14 January 2022
Accepted 17 April 2022

KEYWORDS
ASV; path planning; GNC system; AFSA

1. Introduction

With the development of autonomy technology, there has been a growing appeal for the research of autonomous systems. In particular, much attention is given to autonomous surface vessels (ASVs) due to their potential benefits of improving safety and efficiency. ASVs can be defined as unmanned ships which perform tasks in a variety of cluttered environments without any human intervention. ASVs have already shown their contributions in some areas like ocean research, ocean resource exploration, military, maritime transport and rescue (Zhou et al. 2020). Table 1 shows the examples of ASVs' applications in recent years.

Path planning is one of the key technologies in the process of automating the ASVs and carrying out complex tasks of ASVs (Fossen 2011; Lazarowska 2015). In recent years, there is an increasing demand for maritime safe navigation and path planning technology. According to the Annual Overview of Marine Casualties and Incidents 2019 (EMSA 2019) collected by the European Maritime Safety Agency (EMSA), during 2011–2018, more than 54% of all accidents with ships were navigational accidents. Also, 65.8% of these accidents were attributed to human actions. The high percentage of navigational casualties and human erroneous actions can be largely reduced by introducing path planning algorithms.

Developing path planning algorithms with great computing efficiency, robustness, and higher-quality solutions is an attractive topic in recent studies. Sang et al. (2021) proposed a multiple sub-target artificial potential field (MTAPF) based on traditional APF. The MTAPF can greatly reduce the probability of USVs falling into the local minimum by switching target points. Xie et al. (2019) modified the A* algorithm by combining scalar mode, adaptive step and penalty mode. Compared with the real-case trajectory, the distance to the obstacles increased more than three times and path length is much shorter. Liang et al. (2020) proposed a leader-vertex ant colony optimisation algorithm (LVACO) and applied it to the ASV control system. Simulation results reveal that the route given by the LVACO algorithm is more efficient and suitable for ship navigation. Another attempt was made by Zhong et al. (2021), they combined particle swarm optimisation with orientation angle-based grouping. The modified algorithm showed better performance in converging time and path length. To implement an algorithm to ship autonomous navigation, Lazarowska (2020) used a discrete artificial potential field method combined with COLREGs. The method was validated by using real navigation data from the training ship *Horyzont II*. Guo et al. (2020) proposed a chaotic and sharing-learning particle swarm optimisation (CSPSO) algorithm to solve the multi-objective path planning problem. Simulation experiments validate that the CSPSO algorithm and collision avoidance rules are effective and justifiable.

Furthermore, there is an increasing interest in considering dynamic obstacles and multiple ASVs path planning. To cope with dynamic obstacles, Lyridis (2021) improved the ant colony optimisation (ACO) algorithm with the fuzzy logic method. The path planner considered multi-objectives including travelled distance, path smoothness, and fuel consumption. By using a multi-layer path planner, Wang et al. (2019) solved the ASV path planning problem in complex marine environments including dynamic obstacles and arisen reefs. The B-spline method and stochastic dynamic coastal environment (SDCE) model is built to adapt to the time-varying environments. A new path planning algorithm based on self-organising map (SOM) and fast marching method (FMM) has been proposed by Liu et al. (2019). The algorithm has been verified through a number of multiple USVs simulations and has been proven to work effectively in both simulated and practical maritime environments. To solve the online relative optimal path planning problem of multiple USVs, Wen et al. (2020) improved rapidly extending random tree (RRT*) for path optimisation. The dynamic obstacle avoidance has been investigated based on COLREGs, and the algorithm was proved to be

CONTACT Yong Bai baiyong@zju.edu.cn School of Civil Engineering and Architecture, Zhejiang University, Hangzhou 310058, People's Republic of China

Table 1. Examples of ASVs' applications.

Field	Applications
Scientific Research	Marine biology studies (Katzschmann et al. 2018); Bathymetric survey (Sato et al. 2015); water quality monitoring (Yang et al. 2018)
Ocean Resource Exploration	Oil, gas and mine explorations (Roberts and Sutton 2006; Pastore and Djapic 2010)
Military	Port, harbour and coastal surveillance (Zhao 2018); anti-submarine (Fahey and Luqi 2016)
Other Applications	Transportations and maritime rescue (Shafer et al. 2008; Wilde and Murphy 2018)

relatively easier to execute and lower in fuel expenditure than traditional schemes.

Artificial Fish Swarm Algorithm (AFSA) is a new bionic algorithm imitating the social behaviour of fish in nature, which was first brought by Qian et al. (2002). The algorithm has been used to solve mostly robot or ground vehicle path planning problems while there are very limited researches introducing its application in autonomous vessels. Zhang et al. (2016) adopted the inertia factor to AFSA to improve the convergence rate and accuracy. The experiments were carried out on Pioneer 3-DX mobile robot based on a robot operation system (ROS). To ensure the unmanned ground vehicle's safety in an uncertain environment, Zhou et al. (2021) combined trial-based forward search (TFS) with ASFA. The experiment results have shown the storage efficiency and convergence rate are sufficiently enhanced compared to dynamic programming.

Through the literature review, we have observed a number of limitations in recent studies. They are summarised as follows:

- Many algorithms that appear to be efficient theoretically are not applied and tested in the ship control system, which means they are not convincing in handling real-world situations (Vagale et al. 2021; Table 2).
- In many cases, the simulations do not consider external disturbances such as wind, waves, or currents (Table 2). The modelled environment is not complete, and the performance of the algorithms under real conditions would differ (Huang et al. 2020; Vagale et al. 2021).

Route planning is defined as a macro-modality constraint path planning problem which means its applications are usually in large-scale environments (Zhou et al. 2020). In such circumstances, the ship is assumed to be a particle and we do not consider its specific size constraints and motion dynamics. The solution to this problem is required to be collision-free and efficient in both computing time and path length. Therefore, to cope with these requirements and limitations, an improved IAFSA has been developed. The contributions of this work can be addressed in the following three aspects:

- An improved artificial fish swarm algorithm (IAFSA) is proposed to achieve safe route planning for ASVs, which combines a directional operator, probability weight factor, adaptive operator, and a path smoother to improve the efficiency and feasibility of the algorithm.
- A competitive study between IAFSA and other state-of-the-art algorithms is provided to illustrate the excellent performance of the proposed algorithm.
- A simulation-based sea trial around the Nan Hai area by integrating IAFSA with ship GNC system is carried out to prove its feasibility in real-world situations. Ocean disturbances including wind, waves and current are considered during the trial.

Table 2. Lists of recent studies.

Research	Method	Incorporating with GNC system	Simulations considering wind, waves and currents
Sang et al. (2021)	MTAPF	No	No
Xie et al. (2019)	Improved multi-direction A* algorithm	No	No
Liang et al. (2020)	LVACO	Yes	Yes
Zhong et al. (2021)	Improved PSO	Yes	Yes
Lazarowska (2020)	Discrete APF	No	No
Guo et al. (2020)	CSPSO	Yes	Yes
Lyridis (2021)	Improved ACO	No	No
Wang et al. (2019)	Improved FMM	No	No
Liu et al. (2019)	FMM combining SOM	No	No
Wen et al. (2020)	Improved RRT*	No	No

The paper is organised as follows: Section 2 presents the methodology of IAFSA and its competitive results with other algorithms. In Section 3, a computer-based sea trial around the Nan Hai area has been conducted to present the application of IAFSA in the real ocean environment. Conclusion is addressed in Section 4.

2. Methodology

2.1. Traditional AFSA for route planning

Artificial fish (AF) is a fictitious entity. The AF imitates the social behaviours of real fish to find the position with the best food concentration. The algorithm consists of four behaviours: prey behaviour, follow behaviour, swarm behaviour and random behaviour. The basic idea of these behaviours can be described as follows:

The total population of the fish is N, the position state of each AF is $X = (X_1,\ X_2,\ X_3,\ \ldots,\ X_n)$. $Y = f(X_i)$ denotes the food concentration in the current position. Visual and Step is the maximum range in which AFs can search and move.

2.1.1. Prey behaviour

A basic biological behaviour for fish to find food (Figure 1). The current state of an AF is $X_i(t)$. $X_j(t)$ is the random position state neighbouring the current AF in the range of visual, which can be expressed as (1).

$$X_j(t) = X_i(t) + \text{Visual} \times \text{rand}(0,\ 1) \tag{1}$$

If the food concentration $Y_i > Y_j$, the AF will take a Step in the direction of $X_j(t)$, which is done by

$$X_i(t+1) = X_i(t) + \frac{X_j(t) - X_i(t)}{X_j(t) - X_i(t)} \times \text{Step} \times \text{rand}(0,\ 1) \tag{2}$$

If $Y_i < Y_j$, then $X_j(t)$ will be selected again. If the AF is not satisfied with the forward condition after try_num times, the concerned AF performs random behaviour to avoid the local optimum.

2.1.2. Follow behaviour

Once an AF finds a better position, the neighbour AFs will follow and reach it immediately (Figure 2). Suppose the current

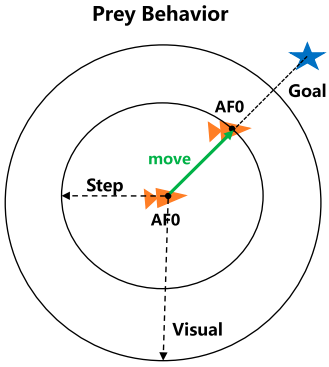

Figure 1. Illustration of prey behaviour. (This figure is available in colour online).

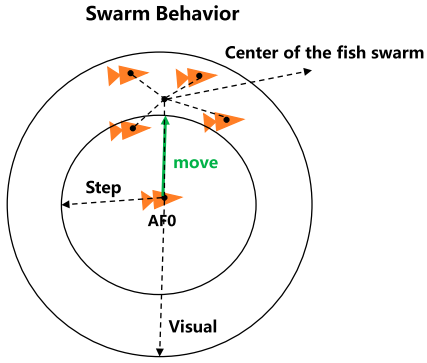

Figure 3. Illustration of swarm behaviour. (This figure is available in colour online).

position of AF is $X_i(t)$, and position $X_j(t)$ denotes the neighbour fish with better food concentration in its visual scope. Swarm centre $X_c(t)$ is defined as the arithmetic average of all AFs' states, see Equation (4). n_f is the number of AFs in the visual scope of the swarm centre. δ denotes the parameter denoting the level of crowds. If $Y_j < Y_i$ and $n_f/N < \delta$, which means position X_j(t) has better food consistency and is not crowded. Then, the AF moves a step in the direction of X_j(t). The expression can be determined as (3)

$$X_i(t+1) = X_i(t) + \frac{X_j(t) - X_i(t)}{X_j(t) - X_i(t)} \times \text{Step} \times \text{rand}(0, 1) \quad (3)$$

if there are no neighbours to be found or the condition is not satisfied, the AF will perform prey behaviour.

2.1.3. Swarm behaviour

In order to keep swarm generality, AFs attempt to move towards the central position at every time of iterations, the swarm behaviour is illustrated in Figure 3. The central position is determined in the following equation:

$$X_c(t) = \frac{1}{N}\sum_{i=1}^{N} X_i(t) \quad (4)$$

n_f is the number of AF swarms in the visual range of $X_c(t)$. If $n_f/N < \delta$ and $Y_c < Y_i$, it means the centre position has better food consistency and the swarm is not crowded, then the AF can take a step in the direction of $X_c(t)$, which is done by

$$X_i(t+1) = X_i(t) + \frac{X_c(t) - X_i(t)}{X_c(t) - X_i(t)} \times \text{Step} \times \text{rand}(0, 1) \quad (5)$$

Otherwise, the AF executes prey behaviour.

2.1.4. Random behaviour

To prevent local optimum, the AF would execute random behaviour if the other behaviours are failed to execute. Random behaviour means the AF chooses an arbitrary state or position randomly in its visual field, and then it swims towards the selected state. It can be described as follows:

$$X_i(t+1) = X_i(t) + \text{Step} \times \text{rand}(0, 1) \quad (6)$$

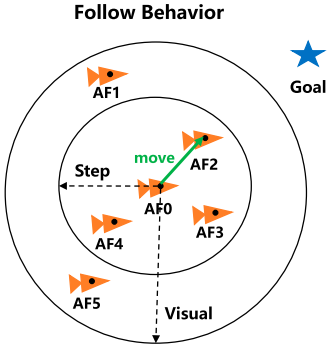

Figure 2. Illustration of follow behaviour. (This figure is available in colour online).

2.2. The improved artificial fish swarm algorithm

2.2.1. Directional operator and probability weight factor

In traditional AFSA, before moving to the next position, AF usually searches for the next state randomly in the range of its visual. There are some drawbacks to this process. First, it is a time-consuming task. AF needs to try all the possible directions until the position is found. Second, the path generated by the prey behaviour is not optimal. Due to the random process, the path quality is greatly influenced by the jagged effect (existence of redundant turns that form like a zigzag).

To overcome these drawbacks, we introduce a heuristic directional operator. During the prey behaviour, the AF is inspired by the operator and consciously chooses the best position by itself. Suppose that $X_{i,j}^p$ represents the potential position number j of AF number i in the step range. P represents the set of all the potential position, which can be expressed as

$$P = \{X_{i,j}^p | X_{i,j}^p - X_i \le \text{Step},\ i = 1, 2, 3, \ldots, N,\ j = 1, 2, \ldots, M\} \quad (7)$$

In prey behaviour, the food concentration of all the potential positions in P is calculated and then the best position $X_{i,\text{best}}^p$ is selected to be the next step, see Equations (8) and (9). The directional operator first guarantees the AF can find the best position with one cycle of calculation, which significantly reduces the computing time. Second, the directional operator replaces the random process; thereby, the redundant turns and unnecessary

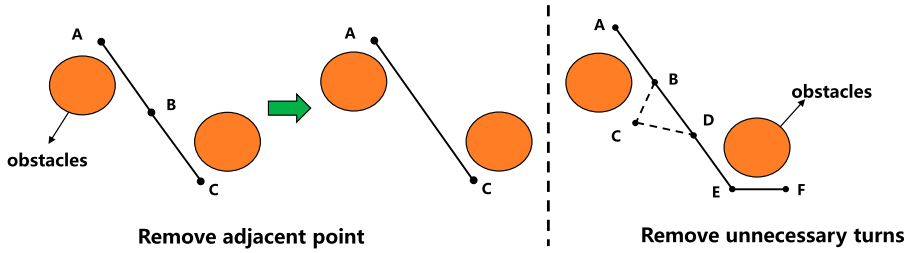

Figure 4. Illustration of waypoint modifying path smoother. (This figure is available in colour online).

nodes are reduced.

$$X^p_{i,\text{best}} = \min\{f(X^p_{i,1}), f(X^p_{i,2}),\ f(X^p_{i,3}),\ \ldots,\ f(X^p_{i,M})\} \tag{8}$$

$$X_i(t+1) = X_i(t) + \frac{X^p_{i,\text{best}}(t) - X_i(t)}{X^p_{i,\text{best}}(t) - X_i(t)} \times \text{Step} \times \text{rand}(0,\ 1) \tag{9}$$

However, after eliminating the random process, the adaptability of the AFSA is weakened. The algorithm is easier to get into local optimum. In order to compensate for it, we introduce a probability weight factor m, which follows the Bernoulli distribution. Therefore, the AF will execute random behaviour to jump out of the local optimum at a certain frequency. Equation (9) is rewritten as (10).

$$X_i(t+1) = \begin{cases} X_i(t) + \dfrac{X^p_{i,\text{best}}(t) - X_i(t)}{X^p_{i,\text{best}}(t) - X_i(t)} \times \text{Step} \times \text{rand}(0,\ 1),\ \ m = 0 \\ X_i(t) + \dfrac{X_j(t) - X_i(t)}{X_j(t) - X_i(t)} \times \text{Step} \times \text{rand}(0,\ 1),\ \ m = 1 \end{cases} \tag{10}$$

2.2.2. Adaptive factor

In standard AFSA, the visual and step are fixed. At the beginning of the algorithm, large values of visual and step leads to better convergence speed. However, when AFs move close to the final position, the large values will cause problems such as local optimum or iterative jumps. But if the values are too small, the efficiency is decreased. Therefore, the algorithm has specific requirements on the size of visual and step in different stages. To balance the global search ability and convergence rate, an adaptive factor is introduced.

Suppose N is the total number of AFs, each AF is recorded as $F_i(i = 1,\ 2,\ 3,\ \ldots,\ N)$. And D_{ij} denotes the distance between two AFs F_i and F_j. The weight factor of the distance D_{ij} is ω_{ij}. Therefore, the visual can be calculated by the weighted average method:

$$V_i = \frac{\sum_{i=1,\, i\neq j}^{N} D_{ij} \times \omega_{ij}}{\sum_{i=1,\, i\neq j}^{N} \omega_{ij}} \tag{11}$$

From Equation (11), we can see the large visual value in the beginning stage will lead AFs move towards positions quickly and make them gathering. As the calculation continues, the visual is gradually getting smaller, which improves the efficiency of searching.

Step is another vital parameter which determines the accuracy of the algorithm. Large step means low accuracy, conversely, small step will improve the accuracy but lead to more time cost. To balance the accuracy and iteration speed, an adaptive step is introduced as (12).

$$\text{Step} = \text{Step} \times \left(1 - \frac{i}{\text{MaxIter}}\right) \tag{12}$$

i denotes the current iteration and MaxIter is the total iterations. From (12), the step is relatively large and the convergence speed is fast at first. As the iteration process, the step gradually gets smaller which leads to an accurate solution.

2.2.3. Waypoint modifying path smoother

The result of traditional method usually contains jags and unnecessary waypoints. Closely placed waypoints and turns will generate extra control demand, which could lead to degraded tracking performance. The path dose not suitable for ship navigation in reality. Therefore, further smoothing method is required. To

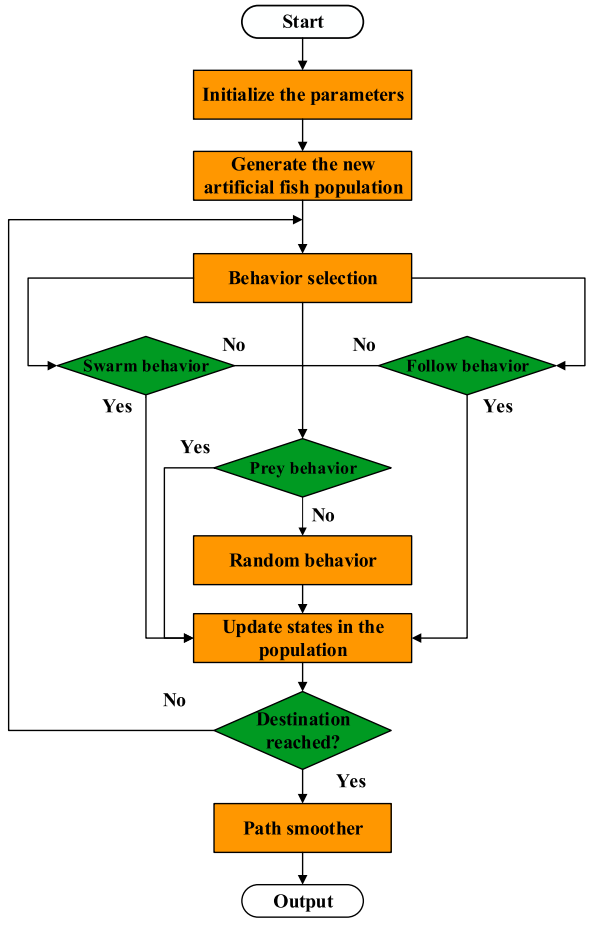

Figure 5. Flow chart of IAFSA. (This figure is available in colour online).

overcome this problem, waypoint modifying path smoother (WMPS) has been adapted.

The method is divided into two steps. (1) Remove the adjacent points if they are colinear. (2) Remove the unnecessary turns if the path does not pass the obstacles. For each iteration, the WMPS checks all waypoints in consecutive three groups: the current waypoint denoted as A; the next via waypoint of A denoted as B; B's via waypoint denoted as C. Figure 4 illustrates how it works. The number of waypoints is reduced and jags are being avoided after modifying. The path generated by WMPS can provide optimum number of waypoints to achieve better control performance for ASV.

The flow chart of Improved artificial fish swarm algorithm is shown in Figure 5.

2.3. Simulation results

This section presents the results of the computer simulations. To verify the effectiveness of IAFSA, four scenarios of grid maps are used and several other algorithms are compared in the simulations. Both starting parameters of IAFSA and AFSA are set to be the same, therefore ensuring the same initial condition. The parameters of ACO are set according to Liang et al. (2020), and we also compare the D* lite algorithm which is presented by Koenig and Likhachev (2005). The simulations are conducted via MATLAB environment with a PC configured with Intel (R) Core (TM) i7-8700 CPU and 8-GB RAM. Moreover, to eliminate the randomness of the algorithms, it should be noted that 100 runs are conducted to obtain a dataset of each scenario.

Figure 6 demonstrates the generated paths by the five algorithms in 10×10 and 20×20 grid maps, respectively. Quantitative results are presented in Table 3, the average value of path length (pixels), the best value of path length (pixels), standard deviation (SD) and average time-consumption (s) are included. It is worth mentioning that the time cost and path length are key factors to reflect the effectiveness and they are presented in bold. Furthermore, the SD, which is defined by Equation (13), reflects the departure degree of dataset from the average, and it is a vital index to evaluate the algorithm's robustness. The best value of the path length generated by IAFSA is presented in bold. Figure 7 presents

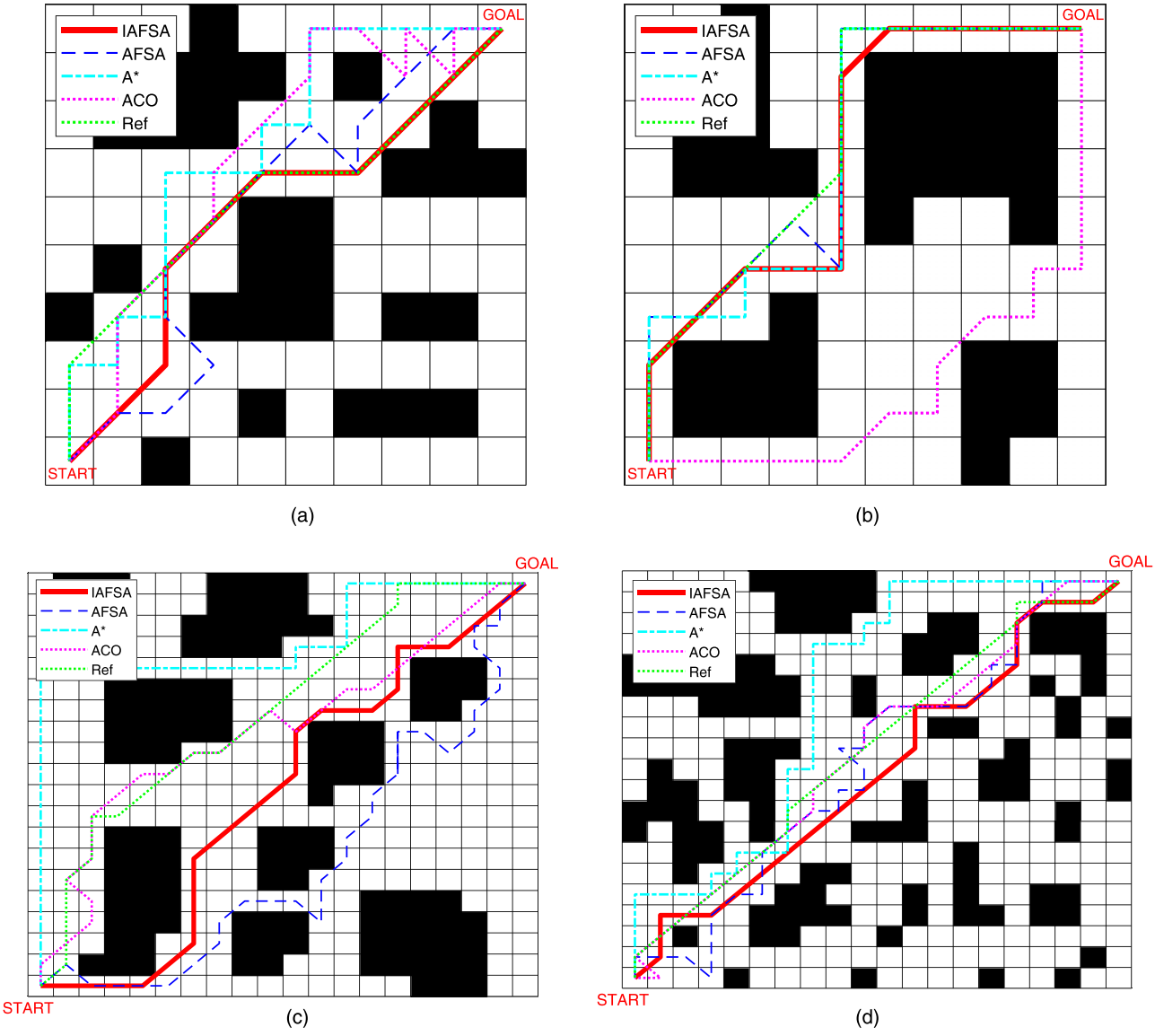

Figure 6. (a) Simulation results of scenario 1; (b) simulation results of scenario 2; (c) simulation results of scenario 3; and (d) simulation results of scenario 4. (This figure is available in colour online).

Table 3. Performance comparison between different methods for four scenarios.

Method	Results	Scenario 1	Scenario 2	Scenario 3	Scenario 4
IAFSA	AVG L (pixels)	14.06	16.26	31.56	30.26
	Best (pixels)	**13.89**	**15.07**	**30.38**	**28.63**
	SD (pixels)	0.39	0.46	0.45	0.49
	AVG T (s)	**0.46**	**0.60**	**1.59**	**1.46**
AFSA	AVG L (pixels)	16.61	17.86	38.97	37.75
	Best (pixels)	15.07	16.24	35.07	31.80
	SD (pixels)	0.72	1.00	1.62	1.57
	AVG T (s)	0.68	0.73	2.23	2.31
ACO	AVG L (pixels)	16.84	16.60	32.97	32.07
	Best (pixels)	15.07	15.07	30.97	29.21
	SD (pixels)	0.94	0.82	0.95	1.19
	AVG T (s)	0.68	0.65	3.14	3.11
A*	AVG L (pixels)	18	18	38	38
	Best (pixels)				
	SD (pixels)	–	–	–	–
	AVG T (s)	0.99	1.11	3.83	4.04
D* lite	AVG L (pixels)	13.89	15.66	30.97	28.63
	Best (pixels)				
	SD (pixels)	–	–	–	–
	AVG T (s)	0.67	0.90	1.71	1.49

the competitive results between different methods.

$$SD = \sqrt{\frac{1}{100}\sum_{i=1}^{100}(L_i - \mathrm{AVG})^2} \tag{13}$$

Overall, the IAFSA have relatively better performance than the others in all the scenarios. As can be seen from Figure 6, IAFSA achieved better solutions in terms of path quality. The lines in blue and green are the paths generated by AFSA and ACO, and a number of zig zags are formed, making it hard for practical use. However, the line in red is obtained by IAFSA, and it gives the routes with fewer waypoints and unnecessary turns, which is more suitable for ASV navigation.

As is shown in Table 3, regarding the length of the generated path, IAFSA gives the optimal in all cases. In particular, the path length is 10–20% shorter in each scenario compared with the conventional AFSA. The shortest path is obtained with the value of 13.9, 15.07, 30.38 and 28.63 pixels, respectively. Also, the superior robustness of IAFSA was shown from the *SD* values of 0.39, 0.46, 0.45, and 0.49 pixels. Meanwhile, the time consumption is significantly reduced due to the directional operator and adaptive operator with the value of 0.46, 0.60, 1.59, and 1.46 s, respectively. In particular, we can observe from the table that the average time cost is almost half of the other algorithms in scenarios 3 and 4.

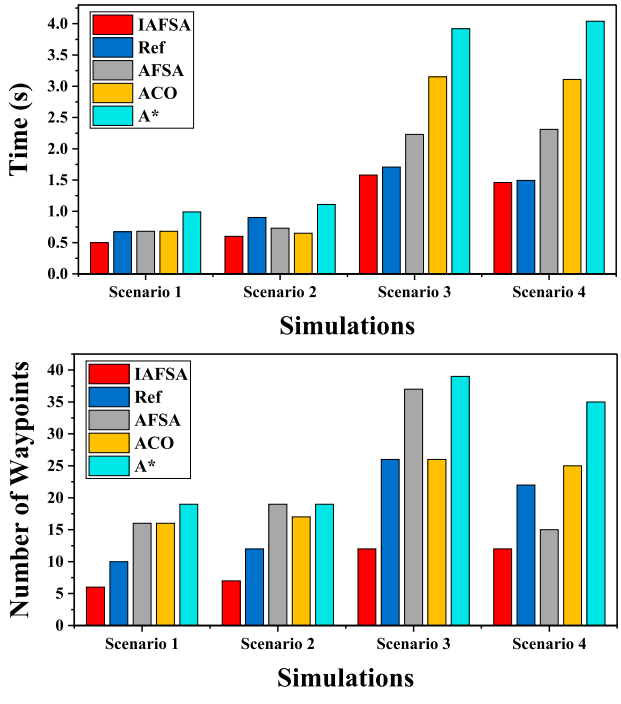

Figure 7. (a) Comparison of computational time; (b) comparison of waypoint number. (This figure is available in colour online).

Figure 8. Model ship. (This figure is available in colour online).

Figure 7 presents the competitive results of the algorithms. As is shown in Figure 7(a), the proposed algorithm achieved better performance in terms of computational time, especially in complex environments such as scenarios 3 and 4. We can also observe that the efficiency of D* lite and IAFSA are relatively close in scenarios 3 and 4. As for the number of waypoints, the waypoints given by IAFSA are significantly less than other competitive algorithms according to Figure 7(b).

3. Computer-based sea trial on GNC system

In this section, the IAFSA is applied to the GNC system in a model ship (Figure 8). The model ship is equipped with a Class 3 DP system to accomplish the mission. It is driven by 8 diesel generators and 12 thrusters. The mathematical model is designed according to Fossen (2011), see Equations (14) and (15).

$$\begin{aligned} \dot{\eta}_p &= \upsilon \\ M\dot{\upsilon} + D\upsilon &= R^T(\psi)b + \tau + \tau_{en} \\ \dot{b} &= 0 \end{aligned} \tag{14}$$

where

$$\tau = Bu \tag{15}$$

In this model, η_p denotes the position vector in vessel parallel coordinates. M and D are mass matrix and damping matrix. The bias vector b is the slowly varying ocean currents, and $R^T(\psi)$ is the transfer matrix between NED coordinate system and body-fixed coordinate system. τ_{en} denotes the environmental forces. The control matrix B describes the thruster configuration while u is the control input vector. It is worth mentioning that the mathematical model is available under the assumption that the vessel moves at a relatively low speed (Fossen 2011).

The configuration of the GNC system in the model ship is illustrated in Figure 9. It contains three basic systems: the guidance system, navigation system and control system. The mission requirement and information about the environment are first sent to the guidance system to generate a map. Then, IAFSA will

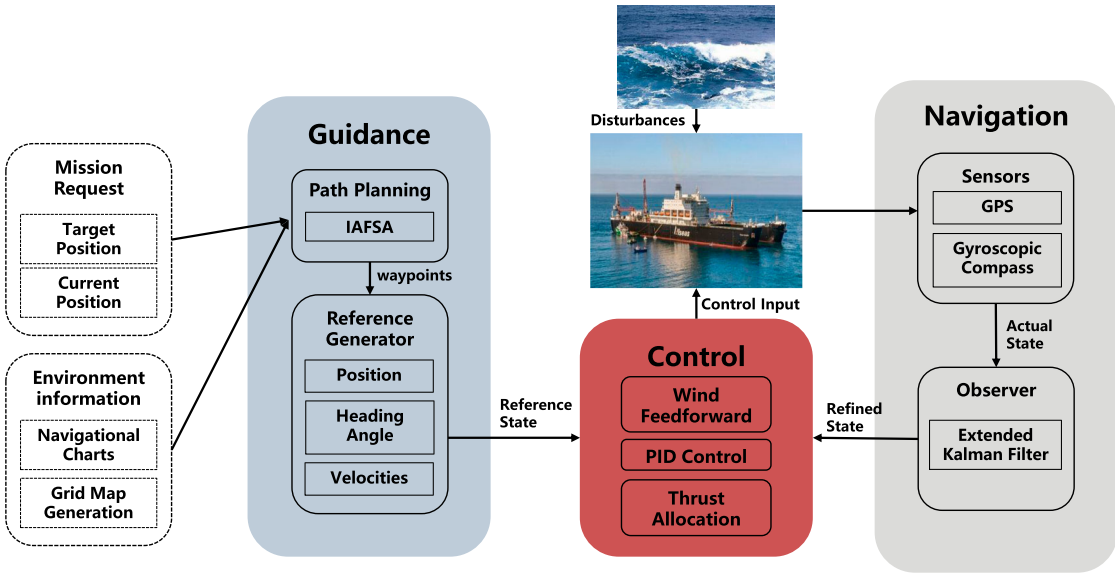

Figure 9. GNC structure of model ship. (This figure is available in colour online).

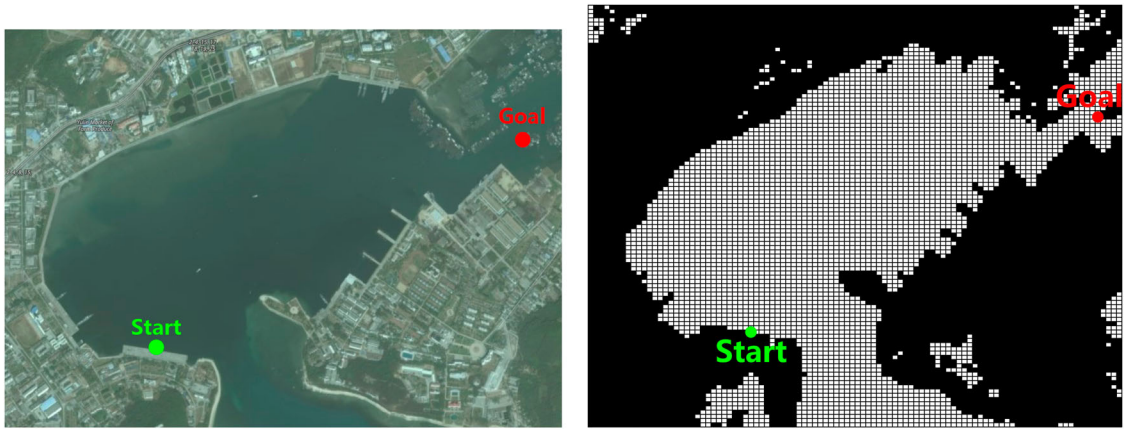

(a) (b)

Figure 10. (a) Satellite map of the sea trial site around Nan Hai area; (b) map after grid process (100 × 100 grid cells, 1 grid cell column length = 22.3 m and row length = 33.5 m). (This figure is available in colour online).

Table 4. Parameter settings.

	Parameters	Value
Environment parameters	Wave Hs	1.5 m
	Wave Tp	14 s
	Wind speed	10 m/s
	Current speed	0.1 m/s
Vessel dynamics	Max speed	0.5 m/s
	Max turn	5°/s
	Max power	11,000 kW

Table 5. Waypoint information.

Waypoint	Coordinate (m)
Start position	(1038.5, 512.9)
Waypoint No. 1	(2613, 1561)
Waypoint No. 2	(2881, 1561)
Waypoint No. 3	(3015, 1650.2)
Goal position	(3216, 1650)

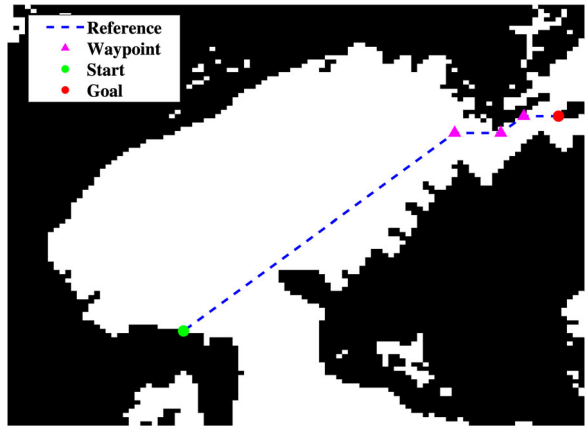

Figure 11. Waypoints and reference trajectory generated by guidance system. (This figure is available in colour online).

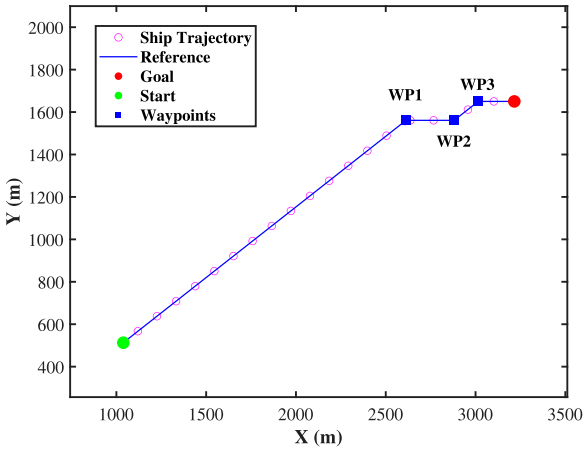

Figure 12. Ship trajectory during the simulation. (This figure is available in colour online).

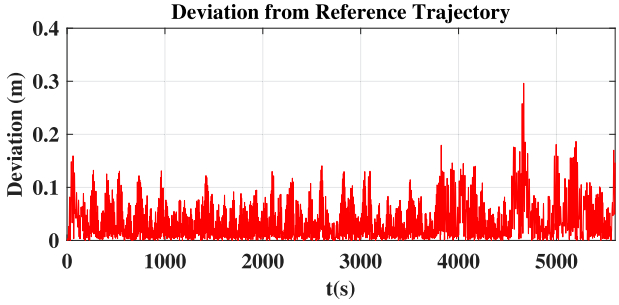

Figure 13. Deviation between real trajectory and reference trajectory. (This figure is available in colour online).

compute a set of waypoints which is a collision-free route for the mission. According to the waypoints and vessel dynamics, the guidance system calculates the reference trajectory and velocity. The reference trajectory is further received by the control system, which includes a PID controller and a thrust allocation system to generate the control commands. The navigation system employs a GPS and gyroscopic compass to measure the position and velocity information. To improve the accuracy of the signal, an extended Kalman filter is designed to refine the signal collected by the sensors.

Sea trials have been carried out in a real sea environment around the Nan Hai area in southern China, and the environment map is shown in Figure 10(a). The start and goal positions have been manually selected (Figure 10(b)). To complete the environment model, it is worth mentioning that the vessel is exposed to environmental disturbances including wind, waves and currents. Also, the vessel dynamics constraints are considered to simulate the real situation. These parameters are shown in Table 4. Once all the parameters are set, the guidance system will first start the offline path planning process to generate waypoints for the mission (Table 5 and Figure 11). And then, the sea trial begins, and the vessel starts at the beginning coordinate (1038.5, 512.9 m) which is marked as a green dot in Figure 10(a). It continuously generates control signals by calculating the error between reference states and actual states observed by the navigation system. After receiving the control input, the thrusters would execute the signal and output forces and moments to follow the route.

Overall, the GNC system with IAFSA has excellent performance executing the sea trial. The vessel autonomously follows the route without any human intervention. Figure 11 and Table 5 present the waypoint coordinates and reference trajectory generated by the guidance system. It is shown in Figure 11 that the route is smooth with three waypoints totally, which makes the trajectory easier to track. Figure 12 shows the simulation results of the model ship; the blue curve is the reference trajectory while the

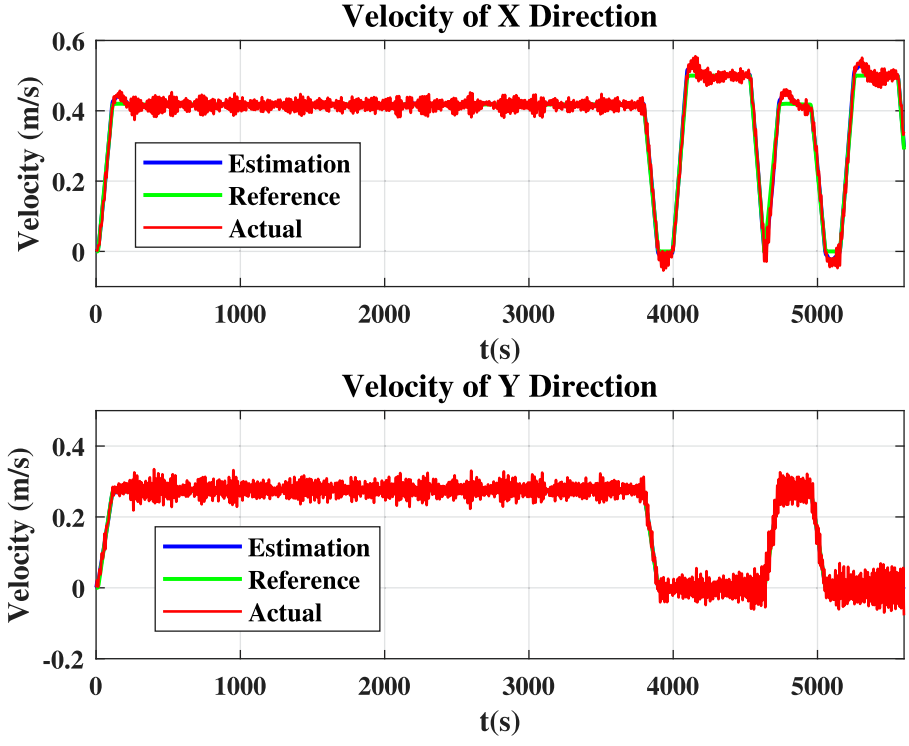

Figure 14. Velocity recorded during the simulation. (This figure is available in colour online).

red circles along this blue curve denote the trace of the model ship. We can see these two elements are basically overlapped on each other. Since it is hard to see the differences between reference route and real trajectory from Figure 12, we present Figure 13 to illustrate the control deviation. As can be seen from the figure, the signal of the tracking error is less than 0.4 m, which means the deviation of the ship's trajectory from the planned path is small even under the effects of environmental disturbances. Additionally, Figure 14 demonstrates the velocity changes during the trial. The blue curve is the velocity signal refined by an extended Kalman filter. The green curve is the reference velocity signal generated by the guidance system while the red curve is the actual velocity. As can be seen from the curves, the vessel is moving at a relatively low speed (0.5 m/s), which is conform to the maximum speed settings. Besides, Figure 14 shows the excellent performance of the navigation system and control system. It can be observed that a relatively large deviation exists when the vessel changed directions. The reason for this is that the thrust forces changed drastically to turn the direction. Overall, the tracking deviation of velocity and position is very small, which means the three subsystems are synchronising well with each other. Therefore, the results of the sea trial provide strong evidence that IAFSA is compatible with the ship control system in the real ocean environment.

4. Conclusion

In this paper, an improved artificial fish swarm algorithm has been proposed, verified and validated by a set of simulations. The algorithm is designed to improve the efficiency and feasibility of path planning of autonomous vessels. Compared with other state-of-the-art algorithms, IAFSA outperforms the others in both algorithm efficiency and path quality. Besides, the path given by IAFSA has fewer unnecessary waypoints and is more suitable for ship navigation. Meanwhile, the IAFSA has been integrated into the GNC system of our model ship. The computer-based sea trials under the disturbances including wind, waves, and currents verify its feasibility in practical application.

In terms of the future work, two main issues can be addressed as follows: (1) Considering the path planning in a dynamic environment. In a real situation, there could be potential danger occurring during the voyage. This requires the ASVs to cope with the time-vary environment. (2) Implementation of practical ASV. The computer-based sea trial was conducted successfully in this study. However, to further prove its feasibility in practical application, experiments on real ASV are still needed in the future.

Acknowledgements

The authors would like to thank the Editor-in-Chief, the Associate Editor, and the anonymous referees for their comments and suggestions. The work is mainly supported by the Institute of Structural Engineering at Zhejiang University. The original code and software we produced are presented on the author's Github page (https://github.com/LiangZhao13) for academic discussion.

Disclosure statement

No potential conflict of interest was reported by the author(s).

References

European Maritime Safety Agency. 2019. Annual overview of marine casualties and incidents 2019. Lisboa: European Maritime Safety Agency. [accessed 2021 Nov 17]. http://www.emsa.europa.eu/newsroom/latestnews/download/5854/3734/23.html.

Fahey S, Luqi X. 2016. Unmanned vehicles for anti-submarine warfare. In: OCEANS 2016 MTS/IEEE Monterey; p. 1–4. DOI:10.1109/OCEANS.2016.7761505.

Fossen T. 2011. Handbook of marine craft hydrodynamics and motion control. DOI:10.1002/9781119994138.

Guo X, Ji M, Zhao Z, Wen D, Zhang W. 2020. Global path planning and multi-objective path control for unmanned surface vehicle based on modified particle swarm optimization (PSO) algorithm. Ocean Eng. 216:107693. DOI:10.1016/j.oceaneng.2020.107693.

Huang Y, Chen L, Chen P, Negenborn RR, Gelder Pv. 2020. Ship collision avoidance methods: state-of-the-art. Saf Sci. 121:451–473. DOI:10.1016/j.ssci.2019.09.018.

Katzschmann RK, DelPreto J, MacCurdy R, Rus D. 2018. Exploration of underwater life with an acoustically controlled soft robotic fish. Sci Robot. 3(16):eaar 3449. DOI:10.1126/scirobotics.aar3449.

Koenig S, Likhachev M.. 2005. Fast replanning for navigation in unknown terrain. IEEE Transactions on Robotics. 21(3):354–363. DOI:10.1109/TRO.2004.838026.

Lazarowska A. 2015. Ship's trajectory planning for collision avoidance at Sea based on Ant colony optimisation. J Navig. 68(2):291–307. DOI:10.1017/S0373463314000708.

Lazarowska A. 2020. A discrete artificial potential field for ship trajectory planning. J Navig. 73(1):233–251. DOI:10.1017/S0373463319000468.

Liang C, Zhang X, Han X. 2020. Route planning and track keeping control for ships based on the leader-vertex ant colony and nonlinear feedback algorithms. Appl Ocean Res. 101:102239. DOI:10.1016/j.apor.2020.102239.

Liu Y, Song R, Bucknall R, Zhang X. 2019. Intelligent multi-task allocation and planning for multiple unmanned surface vehicles (USVs) using self-organising maps and fast marching method. Inf Sci. 496:180–197. DOI:10.1016/j.ins.2019.05.029.

Lyridis DV. 2021. An improved ant colony optimization algorithm for unmanned surface vehicle local path planning with multi-modality constraints. Ocean Eng. 241:109890. DOI:10.1016/j.oceaneng.2021.109890.

Pastore T, Djapic V. 2010. Improving autonomy and control of autonomous surface vehicles in port protection and mine countermeasure scenarios. J Field Robot. 27(6):903–914. DOI:10.1002/rob.20353.

Qian LX, Shao Z, Xin J. 2002. An optimizing method based on autonomous Animats: fish-swarm algorithm. Syst Eng Theor Pract. 22(11):32. DOI:10.12011/1000-6788(2002)11-32.

Roberts GN, Sutton R. 2006. Advances in unmanned marine vehicles. DOI:10.1049/PBCE069E.

Sang H, You Y, Sun X, Zhou Y, Liu F. 2021. The hybrid path planning algorithm based on improved A* and artificial potential field for unmanned surface vehicle formations. Ocean Eng. 223:108709. DOI:10.1016/j.oceaneng.2021.108709.

Sato Y, Maki T, Matsuda T, Sakamaki T. 2015. Detailed 3D seafloor imaging of Kagoshima Bay by AUV Tri-TON2. In: 2015 IEEE Underwater Technology (UT); p. 1–6. DOI:10.1109/UT.2015.7108314.

Shafer AJ, Benjamin MR, Leonard JJ, Curcio J. 2008. Autonomous cooperation of heterogeneous platforms for sea-based search tasks. In: OCEANS 2008; p. 1–10. DOI:10.1109/OCEANS.2008.5152100.

Vagale A, Bye RT, Oucheikh R, Osen OL, Fossen TI. 2021. Path planning and collision avoidance for autonomous surface vehicles II: a comparative study of algorithms. J Mar Sci Technol. DOI:10.1007/s00773-020-00790-x.

Wang N, Jin X, Er MJ. 2019. A multilayer path planner for a USV under complex marine environments. Ocean Eng. 184:1–10. DOI:10.1016/j.oceaneng.2019.05.017.

Wen N, Zhang R, Liu G, Wu J. 2020. Online heuristically planning for relative optimal paths using a Stochastic Algorithm for USVs. J Navig. 73(2):485–508. DOI:10.1017/S0373463319000791.

Wilde GA, Murphy RR. 2018. User interface for unmanned surface vehicles used to rescue drowning victims. In: 2018 IEEE International Symposium on Safety, Security, and Rescue Robotics (SSRR); p. 1–8. DOI:10.1109/SSRR.2018.8468608.

Xie L, Xue S, Zhang J, Zhang M, Tian W, Haugen S. 2019. A path planning approach based on multi-direction A* algorithm for ships navigating within wind farm waters. Ocean Eng. 184:311–322. DOI:10.1016/j.oceaneng.2019.04.055.

Yang TH, Hsiung SH, Kuo CH, Tsai YD, Peng KC, Peng KC, Hsieh YC, Shen ZJ, Feng J, Kuo C. 2018. Development of unmanned surface vehicle for water quality monitoring and measurement. In: Proceedings of 4th IEEE International Conference on Applied System Innovation 2018, ICASI 2018; p. 566–569. DOI:10.1109/ICASI.2018.8394316.

Zhang Y, Guan G, Pu X. 2016. The robot path planning based on improved Artificial Fish Swarm Algorithm. Liu F, editor. Eng. 2016:3297585. DOI:10.1155/2016/3297585.

Zhao S. 2018. USV based on automatic stabilizing function. Ordnance Ind Autom. 37(3):32–35.

Zhong J, Li B, Li S, Yang F, Li P, Cui Y. 2021. Particle swarm optimization with orientation angle-based grouping for practical unmanned surface vehicle path planning. Appl Ocean Res. 111:102658. DOI:10.1016/j.apor.2021.102658.

Zhou C, Gu S, Wen Y, Du Z, Xiao C, Huang L, Zhu M. 2020. The review unmanned surface vehicle path planning: based on multi-modality constraint. Ocean Eng. 200:107043. DOI:10.1016/j.oceaneng.2020.107043.

Zhou X, Yu X, Zhang Y, Luo Y, Peng X. 2021. Trajectory Planning and tracking strategy applied to an unmanned ground vehicle in the presence of obstacles. IEEE Trans Autom Sci Eng. 18(4):1575–1589. DOI:10.1109/TASE.2020.3010887.